Communications

Full-Length Single-Walled Carbon Nanotubes Decorated with Streptavidin-Conjugated Quantum Dots as Multivalent Intracellular Fluorescent Nanoprobes

Massimo Bottini,*[,†,‡,||] Fabio Cerignoli,[†] Marcia I. Dawson,[†] Andrea Magrini,[‡] Nicola Rosato,[§] and Tomas Mustelin[†]

Burnham Institute for Medical Research, 10901 North Torrey Pines Road, La Jolla, California 92037, Department of Environmental, Occupational and Social Medicine, University of Rome Tor Vergata, Via Montpellier 1, 00133 Rome, Italy, INFM and Department of Experimental Medicine and Biochemical Sciences, University of Rome Tor Vergata, Via Montpellier 1, 00133 Rome, Italy, and INFN, Laboratori Nazionali di Frascati, P.O. Box 13, 00044 Frascati, Italy

Received March 3, 2006; Revised Manuscript Received May 15, 2006

We report the formation of a supramolecular luminescent nanoassembly composed of individual or small ropes of full-length, single-walled carbon nanotubes decorated with streptavidin-conjugated quantum dots. The supramolecular luminescent nanoassembly was stably dispersed under physiological conditions and was readily visible by both optical and confocal fluorescent microscopies. Jurkat T leukemia cells were able to internalize the nanoassembly by multivalent CD3 receptor-mediated endocytosis (adsorption by cell). Once internalized by cells, the nanoassembly was found to be transported to lysosomes. These properties should make this supramolecular luminescent nanoassembly an excellent building block for the construction of intracellular polyvalent nanoprobes, mimicking natural viral delivery entities with enhanced loading capacity compared to small molecules.

Introduction

The emerging field of nanomedicine using supramolecular nanoassemblies may permit the development of more effective means for diagnosing and treating malignancies compared to the currently used small molecules. To enhance diagnostic or therapeutic efficacy, supramolecular nanoassemblies must be engineered to function in biologically relevant environments and have multivalent loading capacity for easy detection or effective drug delivery. In the past decade, several types of nanoparticles have been prepared and evaluated for tissue targeting, sensing and imaging, and localized therapy.[1] Often, the chemistry of these nanoparticles has limited their stepwise assembly into multilayered systems and capacity to interact multivalently with cell membrane receptors.

Because of their extraordinary physical, chemical, and mechanical properties, both multiwalled (MW) and single-walled (SW) carbon nanotubes (NT) have been intensely investigated.[2] Their ability to be functionalized and visualized in biological environments using simple fluorescent microscopy has enhanced their potential as biological nanoprobes. For example, both pristine MWNT[3] and oxidized SWNT[4] have been coupled to conventional organic small-molecule fluorophores. Unfortunately, the tethered fluorophores have displayed low quantum yields and short lifetimes in an aqueous environment. Moreover, NT oxidation to permit their covalent functionalization damages the atomic lattice and introduces sidewall defects and breakages. Several groups have reported the noncovalent[5] and covalent[6] decoration of NT with quantum dots (QD). While allowing the preparation of NT-based nanoassemblies with excellent optoelectronic and photonic properties, the linkers used to tether QD either covalently or noncovalently to NT can eventually introduce charge transfer between the two materials that results in fluorescence quenching,[5a,6a,6b] thereby limiting visualization by conventional microscopy. Recently, the nondestructive electrostatically driven decoration of full-length SWNT with QD was accomplished using a surfactant.[7] The resulting nanoassembly was readily visible under light microscopy.

Streptavidin (Str), which is a 64-kDa tetrameric protein having a 5-nm diameter,[8] was found to employ its surface amines to adsorb as a helix onto pristine NT sidewalls.[9] Because of these reports, we investigated whether strepavidin-conjugated quantum dots (Str-QD) could be used to decorate full-length SWNT. The resultant SWNT-streptavidin-quantum dots (SWNT-Str-QD) nanoassembly was fully dispersible in PBS, in contrast to the hydrophobic nature of the pristine NT (Figure 1A,B). These supramolecular nanoassemblies, visible by conventional fluorescent microscope, appeared as individual tubes or small ropes-like aggregates by transmission electron microscope (TEM). To demonstrate that this supramolecular luminescent

* Corresponding author. Fax: (858) 713-6274. Tel: (858) 646-3100 (×3063). E-mail address: mbottini@burnham.org.

[†] Burnham Institute for Medical Research.

[‡] Department of Environmental, Occupational and Social Medicine, University of Rome Tor Vergata.

[§] Department of Experimental Medicine and Biochemical Sciences, University of Rome Tor Vergata.

[||] INFN.

10.1021/bm0602031 CCC: $33.50
Published on Web 06/28/2006

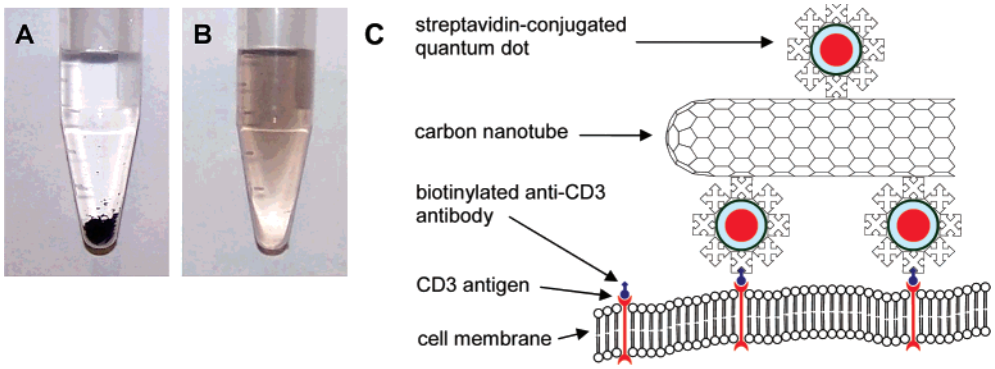

Figure 1. (A and B) Photographs of pristine SWNT (A) and of the dispersable SWNT-streptavidin-quantum dots supramolecular luminescent nanoassembly (B) in phosphate-buffered saline. (C) Schematic showing the interactions between CD3 receptors on the Jurkat T leukemia cell membrane and a SWNT-streptavidin-quantum dots nanoassembly. A biotinylated anti-CD3 monoclonal antibody was used to link CD3 to the nanoassembly. The supramolecular luminescent nanoassembly acted as a multivalent delivery system, with each nanoassembly capable of binding many biotinylated αCD3−CD3 receptor complexes.

nanoassembly could be further functionalized with either small or macromolecules, we exploited the strong affinity between biotin and Str ($K_D = 10^{-15}$ M). We investigated the ability of SWNT-Str-QD to function as a multivalent intracellular fluorescent nanoprobe in Jurkat T leukemia cells to which biotinylated mouse anti-human CD3 antibody (αCD3) bound to surface CD3 receptors. As imaged by confocal microscopy, the CD3 membrane receptor is able to mediate the endocytosis of its ligand, which in this case is the biotin conjugated-αCD3 bound to SWNT-Str-QD (Figure 1C).

Experimental Section

Materials. Pristine SWNT, which were purchased from Carbon Solutions, Inc. (Riverside, CA), were approximately 1.4-nm in diameter and 500−1500-nm long. Str-QD (1 μM in phosphate buffer pH 8), which were purchased from Quantum Dot Corp. (Hayward, CA), consisted of a CdSe−ZnS nanocrystal core coated with a polymer shell that was covalently functionalized with Str. The Str-QD had 525-nm, 605- or 655-nm emission wavelengths. Biotinylated and unconjugated αCD3 were from eBioscience, Inc. (San Diego, CA); normal mouse serum (NMS) was from Santa Cruz Biotechnology (Santa Cruz, CA); normal goat serum (NGS) was from Gibco (Invitrogen Corp., Carlsbad, CA); Alexa Fluor 488-labeled goat anti-rabbit antibody was from Molecular Probes (Invitrogen Corp., Carlsbad, CA); RPMI-1640 cell culture medium and Dulbecco's modified Eagle's medium-high glucose (DMEM-HG) were from Cellgro (Mediatech, Inc., Herndon, VA); fetal bovine serum (FBS) was from Tissue Culture Biologicals (Informagen, Inc., Newington, NH); rabbit anti-human CD107A (LAMP-1) antibody was received from Prof. Fukuda laboratory (Burnham Institute for Medical Research, La Jolla, CA).[10] Poly-L-lysine, formaldehyde, FITC-conjugated concanavalin A, dimethyl formamide (DMF), Triton X-100 and PBS were from Sigma-Aldrich Corp. (St. Louis, MO).

Preparation of SWNT-Str-QD. SWNT were sonicated (model 3510, Branson Ultrasonic Corp., Danbury, CT) at 25 °C for 1 h in DMF to give a uniform dispersion. An aliquot of the dispersion containing 100 μg of NT was washed five times with PBS. The black residue was dispersed in 1 mL of 20 nM Str-QD in PBS, sonicated for 2 h, and then allowed to stand overnight so that undispersed nanotubes sedimented. The resultant clear tan supernatant was carefully collected, filtered through a 0.2-μm polycarbonate-membrane (Poretics Corp., GE Osmonics Labstore, Minnetonka, MN), weighed (approximately 50 μg), and diluted in 1 mL of PBS. The dispersion was subjected to two more rounds of sonication with QD and filtration under the same conditions and finally was redispersed in PBS.

Cell Internalization Studies. Jurkat T leukemia cells were kept in logarithmic growth by culture in RPMI-1640 supplemented with 10% FBS. A total of 5×10^6 cells were washed twice with PBS, incubated for 1 h at 4 °C with 2 μg of (biotinylated or unconjugated) αCD3 in 200 μL of PBS containing 3% NMS. Cells were resuspended in 2 mL of PBS and incubated for 1 h at 4 °C on poly-L-lysine-coated cover slips. HeLa adenocarcinoma cells were seeded onto cover slips and kept in logarithmic grown by culture in DMEM-HG for 24 h and then incubated for 1 h at 4 °C with 2 μg of biotinylated αCD3 in 1 mL of PBS containing 3% NMS. The cover slips were treated with SWNT-Str-QD or Str-QD in PBS for 3 h at 37 °C in 5% CO_2 atmosphere, fixed for 10 min in 3.7% formaldehyde in PBS, and then either stained for 1 h at room temperature with 10 μg/mL FITC-conjugated concanavalin A or incubated with rabbit anti-CD107A and then with Alexa Fluor 488-labeled goat anti-rabbit antibody in PBS containing 5% NGS and 0.1% Triton X-100. VECTASHIELD mounting medium with DAPI (Vector Laboratories, Inc., Burlingame, CA) was used to visualize the nuclear region.

Fluorescent Microscopy. Phase-contrast and fluorescence images of Str-QD and SWNT-Str-QD dispersions were acquired using an Inverted TE300 Nikon (Kanagawa, Japan). Confocal microscopy (Radiance 2100/AGR-3Q, Bio Rad, Hercules, CA) was used to collect fluorescent images after excitation at 488-nm using an argon laser. Both 40× and 60× (1.4-oil immersion) objectives were used. To avoid fluorescence interference from salt crystals caused by evaporation of buffer, wet samples were imaged.

Trasmission Electron Microscopy. An aliquot of SWNT-Str-QD in PBS was dropped onto the lacey carbon film covering a 300-mesh copper grid (Tedpella, Inc., Redding, CA), which was then wiped off after approximately 10 s and air-dried overnight in a desiccator. TEM images were obtained using a Hitachi H-600A (Tokyo, Japan).

Results and Discussion

Both optical and confocal microscopy showed that Str-QD (655-nm emitting) in PBS existed as monodispersed suspension and, therefore, had no distinct fluorescent features (Figure 2).

SWNT-Str-QD in PBS remained as a clear solution without visible flocculation for several days suggesting that the Str-QD-coated pristine SWNT were solubilized by their Str-QD coating as individual or small ropes. Both optical and confocal fluorescent images indicated that the dispersed particles had lateral dimensions mainly below 0.5 μm (Figure 3A,B). Because the diffraction resolution of both optical systems was limited to approximately 250−500 nm (due to the numerical aperture of the objective and condenser lenses) further information about the aspect ratios of the fluorescent features was not possible.

After approximately one week a slight sedimentation was observed in the SWNT-Str-QD dispersion. Fluorescent imaging revealed the sedimented particles had 1−3-μm lateral dimen-

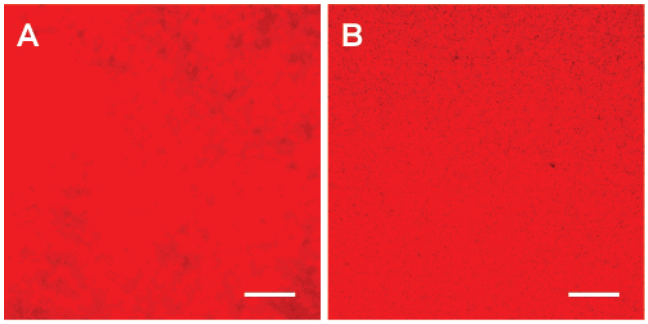

Figure 2. Optical (A) and confocal (B) fluorescent images of the streptavidin-conjugated quantum dots in PBS. That both fields displayed uniform fluorescence suggests that the Str-QD were fully dispersed in PBS, in contrast to Figure 3A,B (scale bar approximately 10 μm).

sions. This slight and slow flocculation suggests that the bigger bundles precipitated. Sedimentation did not increase in the following weeks.

TEM imaging of SWNT-Str-QD showed the presence of SWNT ropes, 10−40-nm in diameter and 0.5−2-μm long, that were decorated with dark particles representing the Str-QD (Figure 3C), supporting the observations made using optical microscopy.

Str-QD with 525- or 605-nm emission wavelength also adsorbed onto SWNT. The TEM and fluorescent (optical and confocal) images of these dispersions revealed both individual/small ropes of Str-QD-coated SWNT (data not shown).

Quantum dots are colloidal single crystals a few nanometers in diameter and are typically coated with functional polymers that permit the tethering of various small and macro-molecules resulting in aqueous environment compatibility. Because of their small size, their energy levels are quantized so that photon energy emission is restricted to a narrow range after broad range absorption. Their adherence to quantum behavior makes them superior to small organic fluorescent molecules that bleach rapidly after excitation only in a narrow absorption range. Str-QD are composed of 5−10-nm (depending on the emission wavelength) CdSe−ZnS nanocrystals coated with 5 nm-diameter Str. The small number of Str, and therefore the biotin-binding sites, on the surface of each Str-QD limits their use as intracellular delivery systems or nanoprobes. In contrast, the extremely high aspect ratio of SWNT make SWNT-Str-QD a better scaffold than Str-QD for constructing intracellular multivalent delivery systems, with each nanoassembly capable of binding many membrane receptors leading to an enhanced activity compared to monovalent drugs.

Recently, the transporting of various types of proteins noncovalently and nonspecifically bound to nanotubes sidewalls through endocytosis into various adherent and nonadherent mammalian cell lines was reported.[2e] We investigated whether SWNT-Str-QD could be used as fluorescently detectable intracellular nanoprobes in Jurkat cells through specific CD3 receptor-mediated endocytosis. Endocytotic uptake pathways are energy-dependent, with optimum uptake occurring at 37 °C and none occurring at 4 °C. Thus incubation of cells with αCD3 was conducted at 4 °C to avoid any αCD3 internalization before treatment with SWNT-Str-QD. Jurkat cells that had been incubated with biotinylated αCD3 at 4 °C and then treated with SWNT-Str-QD at 37 °C had intense internal fluorescence (Figure 4A). Jurkat cells were treated with VECTASHIELD mounting medium with DAPI in order to visualize the nuclear region and to investigate if internalized SWNT-Str-QD reached the nucleus. Intracellular nanoassembly did not overlap the DAPI stained region suggesting that the nanoassembly, after the endocytotic uptake, was not transported to the nucleus (Figure 4B). Further, Jurkat cells were incubated with rabbit anti-CD107A and then with Alexa Fluor 488-labeled goat anti-rabbit antibody in order to visualize the lysosomes, the organelles that serves to digest macromolecules through digestive enzymes. The presence of co-localized red and green features suggested that after the cellular uptake some endocytotic vesicles released the SWNT-Str-QD to the lysosomes (Figure 4C,D).

Jurkat cells that had not been incubated with (biotinylated or unconjugated) αCD3 before the addition of SWNT-Str-QD (data not shown), those incubated with unconjugated αCD3 and then treated with SWNT-Str-QD (at 4 or 37 °C; Figure 4E), or those incubated with biotinylated αCD3 and then treated with SWNT-Str-QD at 4 °C (data not shown) exhibited weak internal fluorescence. We obtained similar results after treatment with Str-QD (data not shown). Moreover, we incubated adherent HeLa cells with biotinylated αCD3 and subsequently with SWNT-Str-QD. Extremely weak internal red fluorescence was observed in few cells (Figure 4F).

These results suggest that without stimulation of the CD3 membrane receptor or in the absence of the CD3 surface receptor (HeLa cells) the endocytotic uptake of the nanoassembly was weak, probably due to nonspecific interactions between the nanoassembly and hydrophobic regions of the cell surface. On the other hand, we observed that the endocytotic uptake of the SWNT-Str-QD was strongly amplified if it occurs by specific CD3 receptor-mediated endocytosis with the biotinylated αCD3 acting as a bifunctional agent to cross-link the CD3 surface receptor to the nanoassembly through biotin-streptavidin binding (Figure 1C). Further, we observed that, once internalized by cells, part of the SWNT-Str-QD was transported to lysosomes. More experiments are in progress to better establish the localization of the nanoassembly after the cellular uptake.

The strong endocytotic uptake of the SWNT-Str-QD fluorescent nanoassembly by the specific CD3 receptor-mediated

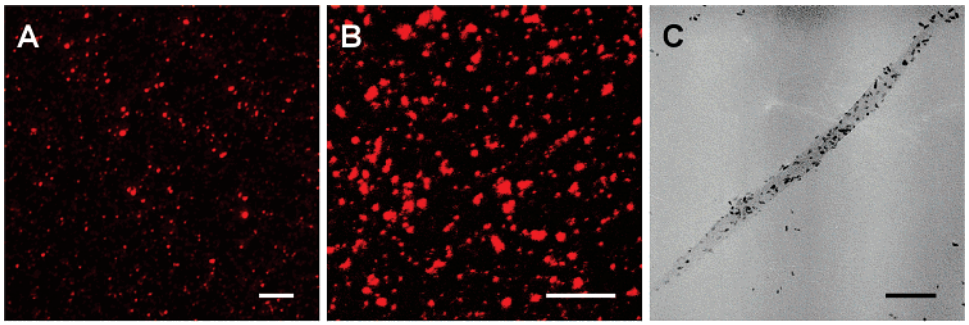

Figure 3. (A and B) Optical (A) and confocal (B) fluorescent images of dispersions of full-length SWNT decorated with Str-QD in PBS (scale bar approximately 10 μm). (C) TEM image of a rope of SWNT coated by Str-QD (scale bar 100 nm).

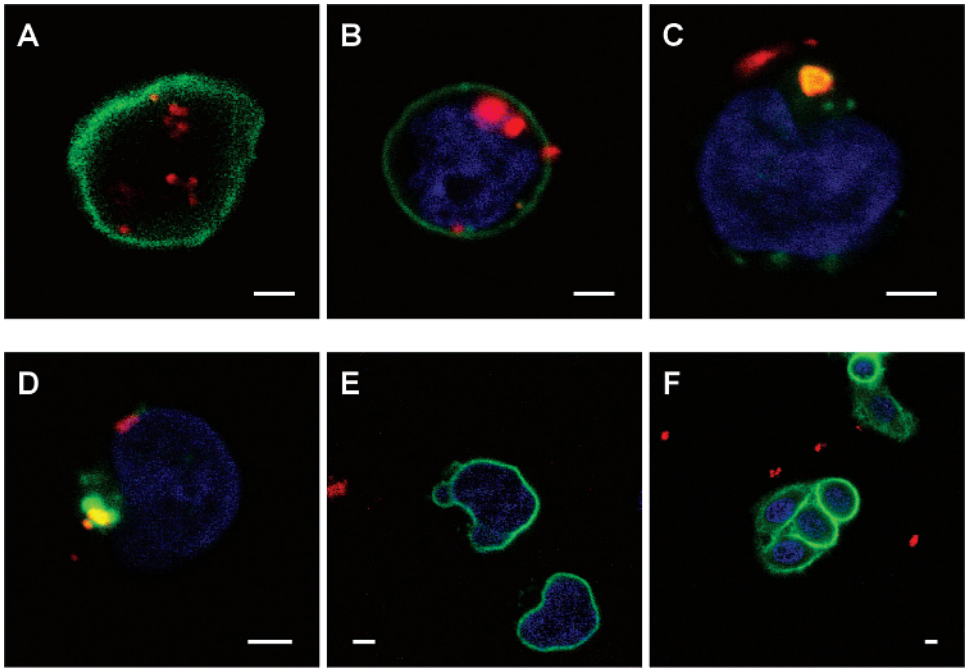

Figure 4. (A) Confocal fluorescent images of SWNT-Str-QD internalized into Jurkat T leukemia cells through biotinylated αCD3-CD3 receptor-mediated endocytosis. (B) Confocal fluorescent images of SWNT-Str-QD internalized into Jurkat T leukemia cells incubated with DAPI (blue) to visualize the nuclear region. (C and D) Confocal fluorescent images of SWNT-Str-QD internalized into Jurkat T leukemia cells incubated with rabbit anti-CD107A and then with Alexa Fluor 488-labeled goat anti-rabbit antibody in order to visualize lysosomes. The co-localization of intracellular nanoassemblies (red) and lysosomes (green) indicate that after CD3 receptor-mediated endocytotic uptake, part of internalized SWNT-Str-QD were transported to lysosomes. (E) Confocal fluorescent images of Jurkat cells incubated with unconjugated αCD3 and then treated with SWNT-Str-QD at 37 °C. (F) Confocal fluorescent images of HeLa cells incubated with biotinylated αCD3 and then treated with SWNT-Str-QD at 37 °C. In images A, B, E and F cell membranes were visualized using FITC-conjugated concanavalin A (green). Scale bars approximately 2 μm.

endocytosis represents an improvement of recently reported intracellular protein transport.[2e] However, before developing any applications both in vitro and in vivo, short- and long-term cytotoxic effects should be accurately established. Indeed, many recently introduced nanoparticles (carbon nanotubes,[11] fullerenes,[12] quantum dots,[13] gold nanoparticles,[14] etc.) have shown signs of toxicity dependent on several factors such as dose, dimension, chemical functionalization, and physical aspect. Moreover, internalization of SWNT−protein conjugates was observed to stimulate dose-dependent apoptosis (programmed cell death).[2e] The fact that the endocytotic uptake is amplified by the stimulation of the CD3 membrane receptor will allow us to use lower concentrations of nanoassembly and probably to decrease the cytotoxic effects with respect to the case without CD3 stimulation. This result could represent an additional improvement compared to previously published cell internalization of SWNT-protein conjugates. More detailed toxicity evaluations are in progress, and they will be reported in future publications.

Conclusions

In conclusion, similar to Str adsorption onto NT sidewalls,[9] we demonstrated that Str-QD was able to adsorb onto the sidewall of full-length SWNT, producing a supramolecular nanoassembly fully dispersible in physiological buffer. As detected by conventional fluorescent microscopy and TEM, the SWNT-Str-QD was composed of Str-QD decorated individual/small ropes of pristine SWNT. This realized supramolecular luminescent nanoassembly was delivered internally into Jurkat T cells through biotinylated-αCD3-CD3 receptor-mediated endocytosis and was partially released to lysosomes. As such, the SWNT-Str-QD complex represents a potentially excellent scaffold for constructing intracellular multivalent nanoprobes.

Acknowledgment. This work was supported by Grant U54 CA119335 from the National Institutes of Health. We thank Dr. Karena Kosco (Burnham Institute for Medical Research, La Jolla, CA) for helpful comments.

References and Notes

(1) (a) Langer, R.; Tirrell, D. A. *Nature* **2004**, *428*, 487. (b) Gao, X.; Cui, Y.; Levenson, R. M.; Chung, L. W. K.; Nie, S. *Nat. Biotechnol.* **2004**, *22*, 969. (c) Haag, R. *Angew. Chem., Int. Ed. Engl.* **2004**, *43*, 278. (d) Salem, A. K.; Searson, P. C.; Leong, K. W. *Nat. Mater.* **2003**, *2*, 668. (e) Kreuter, J.; Ramge, P.; Petrov, V.; Hamm, S.; Gelperina, S. E.; Engelhardt, B.; Alyautdin, R.; von Briesen, H.; Begley, D. J. *Pharm. Res.* **2003**, *20*, 409. (f) Barenholz, Y. *Curr. Opin. Colloid Interface Sci.* **2001**, *6*, 66. (g) Panyam, J.; Labhasetwar, V. *Mol. Pharm.* **2003**, *1*, 77. (h) Bharali, D. J.; Klejbor, I.; Stachowiak, E. K.; Dutta, P.; Roy I.; Kaur, N.; Bergey, E. J.; Prasad, P. N.; Stachowiak, M. K. *Proc. Natl. Acad. Sci. U.S.A.* **2005**, *102*, 11539. (i) Bianco, A. *Expert Opin. Drug Delivery* **2004**, *1*, 57. (f) Akerman, M. E.; Chan, W. C.; Laakkonen, P.; Bhatia, S. N.; Ruoslahti, E. *Proc. Natl. Acad. Sci. U.S.A.* **2002**, *99*, 12617.

(2) (a) Dresselhaus, M. S.; Dresselhaus, G.; Eklund, P. C. *Science of Fullerenes and Carbon Nanotubes*; Academic Press: San Diego, CA, 1996. (b) Endo, M.; Hayashi, T.; Kim, Y. A.; Terrones, M.; Dresselhaus, M. S. *Philos. Transact. A, Math. Phys. Eng. Sci.* **2004**, *362*, 2223. (c) Miyagawa, H.; Misra, M.; Mohanty, A. K. *J. Nanosci. Nanotechnol.* **2005**, *5*, 1593. (d) Kandimalla, V. B.; Tripathi, V. S.; Ju, H. *Biomaterials* **2006**, *27*, 1167. (e) Kam, N. W.; Dai, H. *J. Am. Chem. Soc.* **2005**, *127*, 6021. (f) Katz, E.; Willner, I. *ChemPhysChem* **2004**, *5*, 1084. (g) Rojas-Chapana, J. A.; Giersig, M. *J. Nanosci. Nanotechnol.* **2006**, *6*, 316.

(3) Prakash, R.; Washburn, S.; Superfine, R.; Cheney, R. E.; Falvo, M. R. *Appl. Phys. Lett.* **2003**, *83*, 1219.

(4) Hazani, M.; Naaman, R.; Hennrich, F.; Kappes, M. M. *Nano Lett.* **2003**, *3*, 153.
(5) (a) Li, Q.; Sun, B.; Kinloch, I. A.; Zhi, D.; Sirringhaus, H.; Windle, A. H. *Chem. Mater.* **2006**, *18*, 164. (b) Liu, B.; Lee, J. Y. *J. Phys. Chem. B* **2005**, *109*, 23783.
(6) (a) Banerjee S.; Wong, S. S. *Nano Lett.* **2002**, *2*, 195. (b) Sheeney-Haj-Ichia, L.; Basnar, B.; Willner, I. *Angew.* Chem. Int. *Ed.* **2005**, *44*, 78. (c) Haremza, J. M.; Hahn, M. A.; Krauss, T. D. *Nano Lett.* **2002**, *2*, 1253. (d) Ravindran, S.; Chaudhary, S.; Colburn, B.; Ozkan, M.; Ozkan, C. S. *Nano Lett.* **2003**, *3*, 447. (e) Pan, B.; Cui, D.; He, R.; Gao, F.; Zhang, Y. *Chem. Phys. Lett.* **2006**, *417*, 419.
(7) Chaudhary, S.; Kim, J. H.; Singh, K. V.; Ozkan, M. *Nano Lett.* **2004**, *4*, 2415.
(8) Weber, P. C.; Ohlendorf, D. H.; Wendoloski, J. J.; Salemme, F. R. *Science* **1989**, *243*, 85.
(9) (a) Bradley, K.; Briman, M.; Star, A.; Grüner, G. *Nano Lett.* **2004**, *4*, 253. (b) Balavoine, F.; Schultz, P.; Richard, C.; Mallouh, V.; Ebbesen, T. W.; Mioskowski, C. *Angew. Chem., Int. Ed.* **1999**, *38*, 1912.
(10) Carlsson, S. R.; Roth, J.; Piller, F.; Fukuda, M. *J. Biol. Chem.* **1988**, *263*, 18911.
(11) (a) Bottini, M.; Bruckner, S.; Nika, K.; Bottini, N.; Bellucci, S.; Magrini, A.; Bergamaschi, A.; Mustelin, T. *Toxicol. Lett.* **2006**, *160*, 121. (b) Sayes, C. M.; Liang, F.; Hudson, J. L.; Mendez, J.; Guo, W.; Beach, J. M.; Moore, V. C.; Doyle, C. D.; West, J. L.; Billups, W. E.; Ausman, K. D.; Colvin, V. L. *Toxicol. Lett.* **2006**, *161*, 135. (c) Cui, D.; Tian, F.; Ozkan, C. S.; Wang, M.; Gao, H. *Toxicol. Lett.* **2005**, *155*, 73. (d) Fiorito, S.; Serafino, A.; Andreola, F.; Togna, A.; Togna, G. *J. Nanosci. Nanotechnol.* **2006**, *6*, 591.
(12) Sayes, C. M.; Gobin, A. M.; Ausman, K. D.; Mendez, J. West, J. L.; Colvin V. L. *Biomaterials* **2005**, *26*, 7587.
(13) Derfus, A. M.; Chan, W. C. W.; Bhatia, S. N. *Nano Lett.* **2004**, *4*, 11.
(14) Goodman, C. M.; McCusker, C. D.; Yilmaz, T.; Rotello, V. M. *Bioconjugate Chem.* **2004**, *15*, 897.

BM0602031